Available online at www.sciencedirect.com
ScienceDirect
Journal of Solid State Chemistry 179 (2006) 2799–2804
JOURNAL OF SOLID STATE CHEMISTRY
www.elsevier.com/locate/jssc

Mg-doping experiment and electrical transport measurement of boron nanobelts

K. Kirihara[a,*], H. Hyodo[b], H. Fujihisa[c], Z. Wang[a,1], K. Kawaguchi[a], Y. Shimizu[a], T. Sasaki[a], N. Koshizaki[a], K. Soga[d], K. Kimura[b]

[a]*Nanoarchitectonics Research Center, National Institute of Advanced Industrial Science and Technology, 305-8565 Tsukuba, Japan*
[b]*Department of Advanced Materials Science, The University of Tokyo, 277-8561 Chiba, Japan*
[c]*Research Institute of Instrumentation Frontier, National Institute of Advanced Industrial Science and Technology, 305-8565 Tsukuba, Japan*
[d]*Department of Materials Science, Tokyo University of Science, 278-8510 Chiba, Japan*

Received 30 August 2005; received in revised form 28 December 2005; accepted 10 January 2006
Available online 8 February 2006

Abstract

We measured electrical conductance of single crystalline boron nanobelts having α-tetragonal crystalline structure. The doping experiment of Mg was carried out by vapor diffusion method. The pure boron nanobelt is a p-type semiconductor and its electrical conductivity was estimated to be on the order of 10^{-3} $(\Omega\,\mathrm{cm})^{-1}$ at room temperature. The carrier mobility of pure boron nanobelt was measured to be on the order of 10^{-3} $(\mathrm{cm^2\,Vs^{-1}})$ at room temperature and has an activation energy of ~0.19 eV. The Mg-doped boron nanobelts have the same α-tetragonal crystalline structure as the pristine nanobelts. After Mg vapor diffusion, the nanobelts were still semiconductor, while the electrical conductance increased by a factor of 100–500. Transition to metal or superconductor by doping was not observed.

Keywords: Boron; Nanobelt; $I-V$ characteristics; Gate modulation; Carrier mobility; Mg vapor diffusion; Tetragonal crystal; Hopping conduction

1. Introduction

The one-dimensional nano-structure of boron is promising as various nano-structured devices such as a nano-probe with high strength and a nanowire chemical sensor with high sensitivity because of the thermal stability and mechanical strength of bulk boron. Transport measurement of the boron nanowires is essential in order to clarify the applicability for the nanoscale devices. Recently, various methods for synthesizing boron nanowire were reported [1–4]. Boron nanowires have a variety of structures: amorphous [1], β-rhombohedral crystal [2], α-tetragonal crystal [3], and unknown crystalline phase [4], yet the measurement of their electrical transport is still very limited [5]. We synthesized catalyst-free single-crystalline boron nanobelts (BNBs) using laser ablation [6]. The BNB has four boron icosahedral clusters (BICs) in a unit cell of α-tetragonal boron (α-t-B). We measured the temperature dependences of electrical conductance of the BNB and analyzed them based on a variable range hopping (VRH) system [7]. In this paper, we report the carrier mobility and its temperature dependence and we demonstrate that the conduction mechanism of the BNB can be explained by the hopping system.

The physical properties of the boron-rich solids strongly relate to the bonding nature of the BIC [8]. Based on electronic structure calculations [9,10] and magnetic susceptivity measurement [11], an appropriate carrier doping in bulk boron crystal may produce superconduction with high transition temperatures, which may exceed the transition temperature of MgB_2. The unit cell of the α-t-B has several interstitial atomic sites that can accommodate some metal atoms. We can expect that the doping of metal atoms such as Li or Mg could donate the electrons in a rigid band scheme. Therefore, the metal doping experiment

*Corresponding author. Fax: +81 29 861 4552.
E-mail address: kz-kirihara@aist.go.jp (K. Kirihara).
[1]Present address: Swiss Federal Institute of Technology, Zürich, Switzerland.

0022-4596/$ - see front matter © 2006 Elsevier Inc. All rights reserved.
doi:10.1016/j.jssc.2006.01.015

is effective not only in producing superconduction but also in studying the electronic structure of α-t-B. In this paper, we also report the results of Mg-doping into the BNB by Mg vapor diffusion and the electrical transport measurement of the Mg-doped samples.

2. Experimental

We synthesized the BNB using pulse laser ablation. The detailed synthesis procedure and conditions are described elsewhere [6]. Doping of Mg into BNB was carried out by a vapor diffusion method. Bits of Mg (3 N purity) were placed in a boron nitride (BN) tube. The quartz substrate, on which the BNBs were deposited, and the BN tube were sealed in an evacuated quartz tube. In the quartz tube, the sample substrate was fixed by underlying SiO_2 wool. The quartz tube was heated up to 1073 K and kept for 10 h.

We used micro-fabricated metal electrodes to measure the electrical conductance of BNBs. We dispersed the BNBs into dehydrated ethyl acetate and then dropped them onto a thermally oxidized Si substrate with an oxide-layer (SiO_2) thickness of 500 nm. After drying the wafer and locating the BNB position, bilayer metal electrodes, 5 nm Au on 80 nm Ni, were formed at both ends of the BNB by electron-beam lithography. The current versus bias voltage ($I-V$) characteristics have been measured using an electrometer. We changed the electrical potential of the Si wafer, which acts as a back gate electrode. From the gate voltage modulation for $I-V$ curves, we can study the characteristics of a field effect transistor for the BNBs, from which we can estimate the carrier mobility of the BNBs. The temperature dependence of the conductance was also measured for temperatures from 30 to 420 K.

3. Results and discussion

3.1. Mg vapor diffusion into BNBs

Fig. 1(a) shows a scanning electron microscope (SEM) image of BNBs after Mg vapor diffusion. It is noted that the BNB was not lost in shape after Mg vapor diffusion. The most of the BNB surfaces were smooth. The energy-dispersive X-ray (EDX) spectroscopy of the overall entangled BNBs revealed a signal from Mg. However, oxygen and Si were also detected. The concentration of B, Mg, O, and Si on an average was 98.9, 0.0, 1.1, and 0.0 at% before Mg diffusion, respectively. It changed to 92.4, 2.2, 4.9 and 0.5 at% after Mg diffusion, respectively. We suppose that the origins of slight amount of Si were considered to be quartz substrates, quartz tube and SiO_2 wool put under the sample substrate. Sometimes we observed the growth of cubic particles on the BNBs, as shown in Fig. 1(b). The diffraction pattern of the particles by transmission electron microscope (TEM) clearly indicated that of crystalline MgO. The TEM image of an individual BNB after Mg vapor diffusion is shown in Fig. 1(c). As shown in the inset of Fig. 1(c), the diffraction

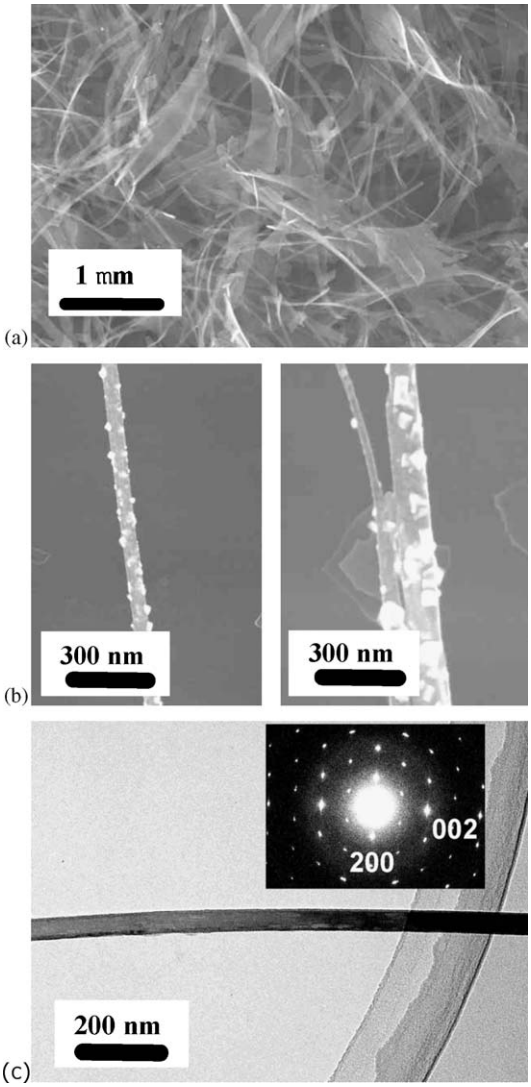

Fig. 1. (a) SEM micrographs of BNBs after Mg vapor diffusion, entangled BNBs. (b) SEM micrographs of small particles with a diameter of several tens nm grown on the surface of BNBs. (c) TEM micrograph of an individual BNB after Mg vapor diffusion. The inset shows the diffraction pattern from this nanobelt. The indices are based on the crystalline structure of α-t-B.

pattern of the individual nanobelt demonstrated that the BNB after Mg vapor diffusion has the same α-t-B structure as the pure BNBs. In addition, EDX spectra installed in the TEM also revealed a signal from Mg together with oxygen and silicon. A ratio of atomic concentrations of Mg, O, Si was approximately 5:8:1 on average. This ratio is comparable to that estimated from the EDX spectra installed in the SEM and matches the existence of MgO and SiO_2 in nearly equal amounts. However, we could not deny that boron oxide layer also could be formed at the surface during vapor diffusion. Assuming the existence of the boron oxide layer and taking the accuracy of the EDX analysis (~1.0 at%) into account, slight amount of atomic Mg or Si can be expected to remain and diffuse into the

nanobelts. The diffusion of Mg or Si into the nanobelts can be expected by the result of the similar vapor diffusion experiment of Mg into β-rhombohedral boron (β-r-B) performed by Soga et al. [11]. They used the powder samples with a particle diameter of several tens μm and successfully doped a few atomic percent of Mg and then confirmed its occupation of interstitial sites in β-r-B crystalline lattice by Rietveld analysis. They detected also a few atomic percent of Si in the β-r-B and concluded that the source of Si may be the quartz tube because Mg is a strong reducer and quartz should be reduced to form atomic Si. In this paper, we employed the same apparatus and similar condition for the vapor diffusion into nanobelts. Considering large difference in the sample size between β-r-B powder (diameter of several tens μm) and our nanobelts (thickness of 20–25 nm), we believe that Mg or Si could diffuse into the crystalline α-t-B of the nanobelt core. As we mentioned, a few percent of metal atom doped into β-r-B can increase the electrical conductivity [15]. We think that the same thing occurred in the nanobelts as we observed significant increase in the conductivity (Fig. 4(b)). We use hereafter the name, 'Mg-doped BNBs', as the name of BNB samples after Mg vapor diffusion.

Recently, several groups reported that the Mg vapor diffusion into boron nanowires lead to the formation of MgB_2 nanowires and $Mg_{0.1}B$ nanowire indicating superconductivity [12–14]. However, our samples of the BNB did not transform into the MgB_2 phase. The different result might be due to the differences in the experimental conditions, such as an annealing temperature, the crystalline structures of boron nanowires, and use of nanowire template material. The other groups chose the temperatures of 1123–1223 K which is higher than that of our case (~1073 K). And Wu et al. [12] and Cao et al. [13] used amorphous boron nanowires. Yang et al. [14] prepared MgB_2 from boron nanorods, which have the same α-t-B as the BNB, but they used the anodic alumina templates and the intermediate product of $AlMg_2O_4$ may result in the different reactions from our study.

3.2. Electrical transport mechanism in the pure (undoped) BNBs

Fig. 2(a) illustrates FE-SEM images of the BNBs with micro-fabricated electrodes. It should be noted that the metal electrodes of the Ni/Au bilayer were clearly developed on both ends of the BNB. Fig. 2(b) compares the $I-V$ characteristics of pure BNB measured at temperatures from 200 to 420 K. The slope of the $I-V$ curve that signifies conductance decreased with decreasing temperature, demonstrating that the BNB was a semiconductor. The value of electrical conductivity, σ, at room temperature estimated without considering a contact resistance between BNB and electrodes was on the order of 10^{-3} $(\Omega\,\mathrm{cm})^{-1}$. The high-resolution TEM observation confirmed that the surface of BNB was covered by amorphous layer with a thickness of only 1–2 nm [6]. This

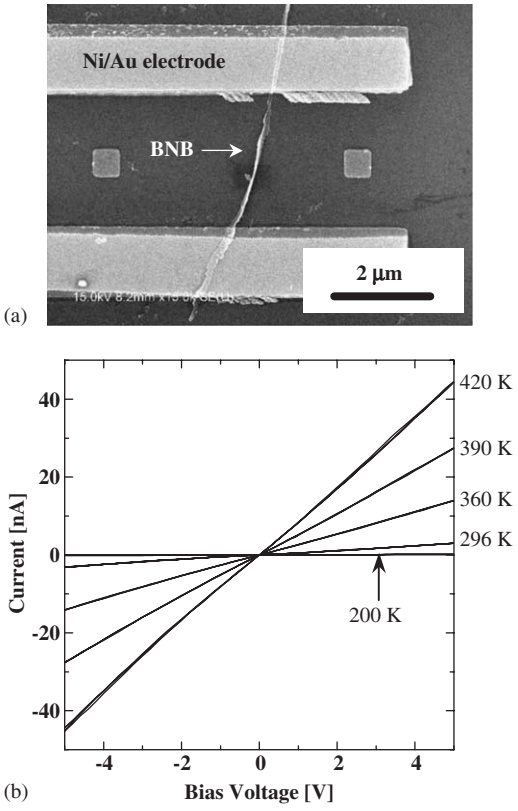

Fig. 2. (a) SEM micrographs of BNB after Ni/Au electrode fabrication. (b) $I-V$ characteristics of this nanobelt at temperatures from 200 to 420 K.

surface layer may consist of the mixture of amorphous boron and boron oxide. In our study, the surface layer did not possess a large contact resistance because rapid annealing of the sample in vacuum (up to 500 K) to improve the contact did not significantly change the $I-V$ curve. The order of magnitude of the conductivity is considered to be valid. This value was comparable to or 10 times larger than that reported by Wang et al. [5] and almost 1000 times higher than those of bulk β-r-B [15].

We have measured the $I-V$ curves as a function of gate voltage (V_g) as shown in Fig. 3(a). Application of negative gate voltage progressively increases the conductance, which signifies a p-type field effect transistor. Therefore, the pure BNB is a p-type semiconductor as well as most of the other pure boron crystals. The carrier mobility of the BNB can be estimated from the gate modulation characteristics with the relation, $\mathrm{d}I/\mathrm{d}V_g = \mu(C/L^2)V$, where μ is the carrier mobility and L is the BNB length (2800 nm) [16,17]. The capacitance, C, is given by $C \sim 2\pi\varepsilon\varepsilon_0 L/\ln(4t/d)$, where t is the thickness of the SiO_2 layer (500 nm), ε is the dielectric constant of SiO_2 layer (~4) and d is the average diameter of the BNB (~50 nm). The room-temperature carrier mobility was estimated to be approximately $3\times10^{-3}\,\mathrm{cm^2\,Vs^{-1}}$ at a bias voltage of $V = 5$ V. The value is comparable to that of bulk β-r-B, while it is significantly smaller than that of α-rhombohedral boron (α-r-B, $\mu \sim 100\,\mathrm{cm^2\,Vs^{-1}}$, at room

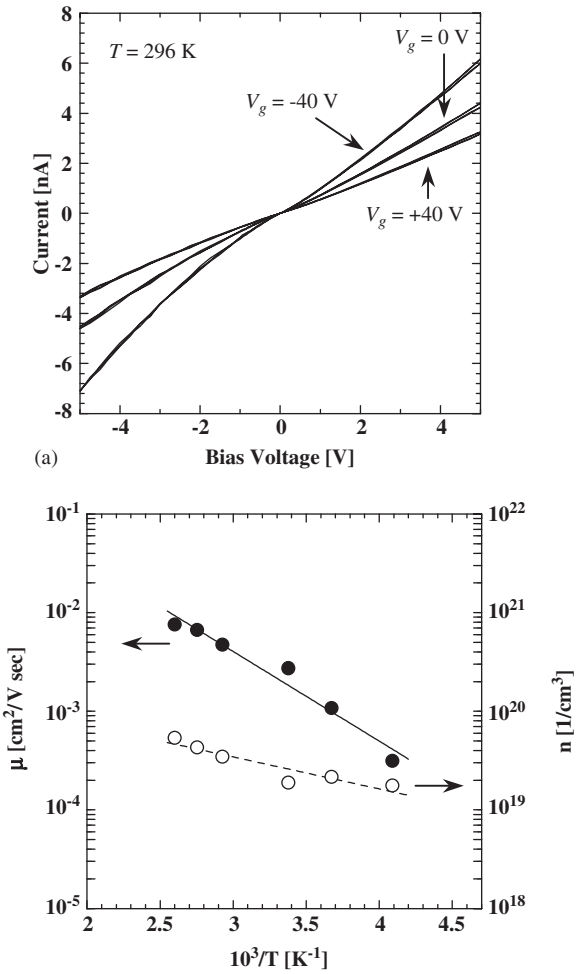

Fig. 3. (a) $I-V$ characteristics of pure BNB at 296 K as a function of the gate voltage of the Si substrate. (b) Carrier mobility and carrier concentration of pure BNB as a function of temperature.

temperature) [8]. The annealing effect mentioned above can contribute again to reduce the surface potential barrier. Wang et al. [5] concluded that rapid annealing of the boron nanowire device at 678 K resulted in the atomic diffusion of Ni from electrode to nanowire entirely and lost the gate modulation behavior by a heavy carrier doping. Since the annealing temperature in our study was approximately 500 K, the diffusion length of atomic Ni may be shorter than that reported by them. The atomic Ni can diffuse only into the surface layer and consequently reduces the contact resistance and surface potential because we observed the gate modulation characteristics even after the annealing. Therefore, we think that the effect of surface coverage on the gate modulation is not significant and the order of magnitude of the mobility is also considered to be valid. The carrier concentration, n, which is estimated from $n = \sigma/e\mu$, is on the order of 10^{19} $(\mathrm{cm})^{-3}$. Furthermore, we measured a temperature dependence of the gate modulation characteristics. The estimated μ and n are shown as a function of temperature in Fig. 3(b). Activation energy of μ and n were estimated to be approximately 0.19 and 0.07 eV, respectively. Both μ and n increase with increasing temperature, while the temperature coefficient of μ is 2–3 times larger than that of n. These properties resemble those of a hopping-conduction system such as β-r-B and differ from those of standard intrinsic semiconductors like α-r-B. In this study, however, we cannot determine a type of hopping conduction because a fitting of the conductance based on the three-dimensional VRH conduction was a little bit better than that by the thermal activation type conduction. We should continue to measure the $I-V$ data and its gate modulation for more BNBs than this study in detail.

3.3. The I–V characteristics after Mg doping

The metal electrodes of the Ni/Au bilayer were also clearly developed on both ends of the Mg-doped BNB (Fig. 4(a)).

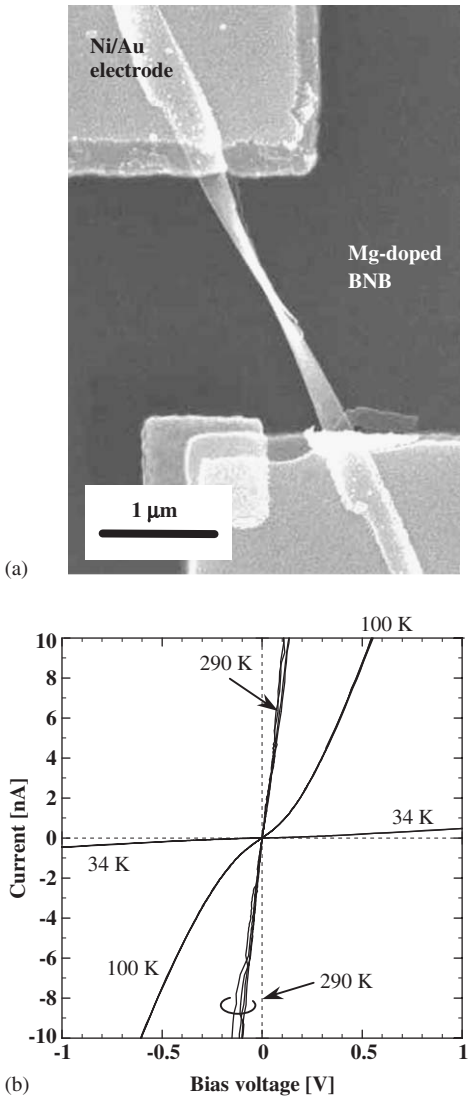

Fig. 4. (a) SEM micrographs of Mg-doped BNB after Ni/Au electrode fabrication. (b) $I-V$ characteristics of this nanobelt at temperatures from 34 to 290 K.

Fig. 4(b) illustrates $I-V$ curves of Mg-doped BNB for temperatures from 34 to 290 K. The slope of the $I-V$ curve decreases with decreasing temperature, indicating that the Mg-doped BNB was also a semiconductor. In particular, the electric current was very small even at the temperature of 34 K, which is lower than the transition temperature of superconductor, MgB_2 [18]. It means that the formation of MgB_2 phase in the BNB did not occur as we mentioned in Section 3.1. We should take care about the contact resistance of Mg-doped nanobelts because the surface layer includes MgO or SiO_2 phase after vapor diffusion experiment and is more important than in the undoped ones. The surface potential barrier might be observed as nonlinear $I-V$ curve at low bias voltage ($|V|<0.2(V)$) shown in Fig. 4(b). However, slopes of the $I-V$ curve at high bias voltage ($|V|>0.2(V)$) signifies large conductance of the nanobelt core (Mg and Si-doped tetragonal boron), which is at least 100 times larger than that of the undoped samples at room temperature. We roughly estimated the conductivity to be on the order of 10^{-1} $(\Omega\,\mathrm{cm})^{-1}$ at 290 K.

We show the temperature dependence of electrical conductance, G, of both pure and Mg-doped BNBs as $\log(G)$ versus $T^{-1/4}$ plot in Fig. 5. In the case of pure BNBs, all of the samples revealed a linear curvature and can be fitted by the VRH model. On the other hand, however, the Mg-doped BNBs revealed a complicated behavior. One of the samples showed a deviation from the linear curvature at $1000/T^{-1/4}>1.4$ ($T<260$ K). The crystalline structure of the BNBs did not change after Mg vapor diffusion as we demonstrated by the TEM. However, we cannot explain the conduction mechanism in the Mg-doped BNBs since we did not measured successfully the carrier mobility of them. The difficulty is also due to lack of the information about the Mg and Si distribution. We are improving the Mg-doping experiment, in particular, preventing the oxidation of BNB and Si atom diffusion. Furthermore, an analysis of crystalline structure Mg-doped BNBs using X-ray diffraction with good statistics will also be necessary to clarify the doping effect.

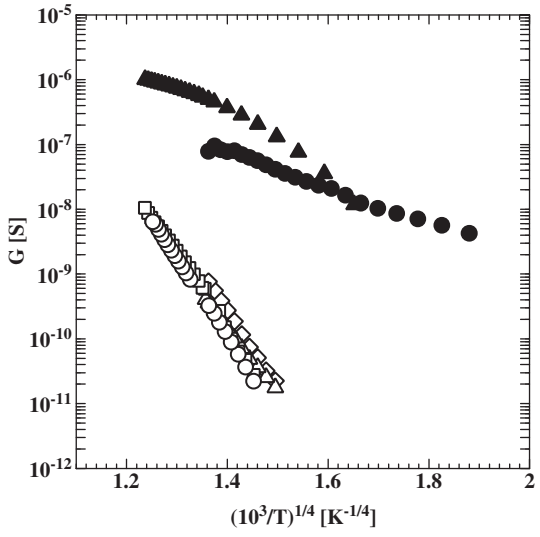

Fig. 5. Temperature dependence of conductance shown as $\log(G)$ versus $T^{-1/4}$ plot. The empty symbols (circles, square, triangle, and diamond) represent the pure BNBs. The solid circle and triangle represent the Mg-doped BNBs.

4. Conclusions

We observed the ohmic $I-V$ characteristics in single-crystal BNBs having α-tetragonal crystalline structure before and after Mg vapor diffusion. The pure (undoped) boron nanobelt is a p-type semiconductor and its electrical conductivity was estimated to be on the order of 10^{-3} $(\Omega\,\mathrm{cm})^{-1}$ at room temperature. We obtained an evidence of hopping conduction system that the carrier mobility of pure BNB was measured to be on the order of 10^{-3} $(\mathrm{cm^2\,Vs^{-1}})$ at room temperature and has an activation energy of ~0.19 eV. The Mg-doped BNBs have the same α-tetragonal crystalline structure as the pure nanobelts. After Mg vapor diffusion, the nanobelts were still semiconductor, while the electrical conductance increased by a factor of 100–500 at room temperature. The $I-V$ curves of Mg-doped BNB revealed that formation of any metallic phase and superconductor MgB_2 phase was not observed.

Acknowledgments

Part of this work was conducted at the AIST Nano-Processing Facility, supported by the "Nanotechnology Support Project" of the Ministry of Education, Culture, Sports, Science and Technology (MEXT), Japan. This work was financially supported by a Grant-in-Aid for Scientific Research from MEXT and JSPS, Japan.

References

[1] L.M. Cao, Z. Zhang, L.L. Sun, C.X. Gao, M. He, Y.Q. Wang, Y.C. Li, X.Y. Zhang, G. Li, J. Zhang, W.K. Wang, Adv. Mater. 13 (2001) 1701–1704.
[2] Y.Q. Wang, X.F. Duan, Appl. Phys. Lett. 82 (2003) 272–274.
[3] T.T. Xu, J.G. Zheng, N. Wu, A.W. Nicholls, J.R. Roth, D.A. Dikin, R.S. Ruoff, Nano Lett. 4 (2004) 963–968.
[4] C.J. Otten, O.R. Lourie, M.F. Yu, J.M. Cowley, M.J. Dyer, R.S. Ruoff, W.E. Buhro, J. Am. Chem. Soc. 124 (2002) 4564–4565.
[5] D. Wang, J.G. Lu, C.J. Otten, W.E. Buhro, Appl. Phys. Lett. 83 (2003) 5280–5282.
[6] Z. Wang, Y. Shimizu, T. Sasaki, K. Kawaguchi, K. Kimura, N. Koshizaki, Chem. Phys. Lett. 368 (2003) 663–667.
[7] K. Kirihara, Z. Wang, K. Kawaguchi, Y. Shimizu, T. Sasaki, N. Koshizaki, K. Soga, K. Kimura, Appl. Phys. Lett. 86 (2005) 212101-1-3.
[8] H. Werheit, R. Schmechel, Boron, in: O. Madelung (Ed.), Landolt–Bornstein New Series, Group III, vol. 41C, Springer, Berlin, 1998, pp. 3–148.
[9] S. Gunji, H. Kamimura, Phys. Rev. B 54 (1996) 13665–13673.
[10] M. Calandra, N. Vast, F. Mauri, Phys. Rev. B 69 (2004) 224505-1-5.
[11] K. Soga, A. Oguri, S. Araake, M. Terauchi, A. Fujiwara, K. Kimura, J. Solid State Chem. 177 (2004) 498–506.
[12] Y. Wu, B. Messer, P. Yang, Adv. Mater. 13 (2001) 1487–1489.

[13] Q. Yang, J. Sha, X. Ma, Y. Ji, D. Yang, Supercond. Sci. Technol. 17 (2004) L31–L33.
[14] L. Cao, Z. Zhang, H. Wen, W. Wang, Appl. Phys. Lett. 86 (2005) 123113-1-3.
[15] H. Matsuda, T. Nakayama, K. Kimura, Y. Murakami, H. Suematsu, M. Kobayashi, I. Higashi, Phys. Rev. B 52 (1995) 6102–6110.
[16] S.M. Sze, Physics of Semiconductor Devices, Wiley, New York, 1981.
[17] Z.L. Wang, Nanowires and Nanobelts: Materials, Properties and Devices, Kluwer Academic Publishers, Dordrecht, 2003.
[18] J. Nagamatsu, N. Nakagawa, T. Muranaka, Y. Zenitani, J. Akimitsu, Nature (London) 410 (2001) 63–64.